Journal of Integrative Agriculture 2019, 18(7): 1460–1472

Available online at www.sciencedirect.com

ScienceDirect

RESEARCH ARTICLE

Transcriptomic analyses reveal new genes and networks response to H5N1 influenza viruses in duck (*Anas platyrhynchos*)

HUANG Yin-hua[1*], FENG Hua-peng[2*], HUANG Li-ren[2*], YI Kang[3], RONG En-guang[1], CHEN Xiao-yun[4], LI Jian-wen[3], WANG Zeng[2], ZHU Peng-yang[2], LIU Xiao-juan[1], WANG Xiao-xue[1], HU Jia-xiang[1], LIU Xin[3], CHEN Hua-lan[2], WANG Jun[3], LI Ning[1]

[1] *State Key Laboratory for Agrobiotechnology, China Agricultural University, Beijing 100193, P.R.China*

[2] *State Key Laboratory of Veterinary Biotechnology, Harbin Veterinary Research Institute, Chinese Academy of Agricultural Sciences, Harbin 150069, P.R.China*

[3] *BGI-Shenzhen, Shenzhen 518083, P.R.China*

[4] *China Veterinary Culture Collection Center, China Institute of Veterinary Drug Control, Beijing 100081, P.R.China*

Abstract

H5N1 influenza represents one of the great challenges to public health. Some H5N1 viruses (i.e., A/goose/Hubei/65/05, GS/65) are weakly pathogenic, while the others (i.e., A/duck/Hubei/49/05, DK/49) are highly pathogenic to their natural hosts. Here, we performed brain and spleen transcriptomic analyses of control ducks and ones infected by the DK/49 or the GS/65 H5N1 virus. We demonstrated that, compared to the GS/65 virus, the DK/49 virus infection changed more numerous immune genes' expression and caused continuous increasing of immune pathways (i.e., RIG-I and MDA5) in ducks. We found that both H5N1 virus strains might escape or subvert host immune response through affecting alternative translation of immune genes, while the DK/49 virus seemed to induce alternative translation of more immune genes than the GS/65 virus. We also identified five co-expressional modules associated with H5N1 virus replication through the weight correlation network analysis (WGCNA). Moreover, we first demonstrated that the duck *BCL2L15* and *DCSTAMP* in one of these five modules inhibited both the highly pathogenic and weakly pathogenic H5N1 virus replication efficiently. These analyses, in combination with our comprehensive transcriptomic data, provided global view of the molecular architecture for the interaction between host and H5N1 viruses.

Keywords: duck, innate immune genes, H5N1 influenza viruses, transcriptomes

1. Introduction

Influenza spreads around the world in seasonal epidemics, resulting in about three to five million cases of severe illness and about 250 000 to 500 000 deaths each year (http://www.who.int/mediacentre/factsheets/fs211/en/). Ducks serve as one of the principal natural reservoir for influenza viruses and harbor all of the known 18 hemagglutinin (HA) and 11

Received 22 January, 2019 Accepted 31 January, 2019
Correspondence HUANG Yin-hua, E-mail: cauhyh@cau.edu.cn
[*] These authors contributed equally to this study.

doi: 10.1016/S2095-3119(19)62646-8

neuraminidase (NA) subtypes of influenza A viruses (IAVs), with exception of the H13, H16–18 and N10–11 subtypes (Deng *et al*. 2013, 2015; Tong *et al*. 2013; Zhu *et al*. 2013). These IAVs are usually nonpathogenic in ducks. However, reassortant and mutant of H5N1 avian influenza viruses (AIs) changed their virulence, even acquired the ability to kill ducks (Song *et al*. 2011). For example, the GS/65 virus shed relative low level of virus titer on day 1, causing fever and body weight loss in ducks (Appendices A and B). While the DK/49 virus is fatal to ducks: 9 of 16 ducks died, two developed severe neurological ataxia and torticollis (Appendix C) (Song *et al*. 2011). Until now, H5N1 virus has caused unprecedented outbreaks in poultry in more than 60 countries and can occasionally cause human infection. As of December 2018, H5N1 virus has caused 860 human infection, with an overall case-fatality of 52% (http://www.who.int/influenza/human_animal_interface/2018_09_21_tableH5N1.pdf?ua=1). Recently, it was reported that an engineered influenza virus based on HA from the highly pathogenic avian influenza A/H5N1 virus can be transmitted between guinea pigs, emphasizing the potential for a human pandemic to emerge from birds (Gao *et al*. 2009; Zhang *et al*. 2013). The exceptional virulence of AIs in human, therefore, motivates us to better understand the host immune response to AIs.

The transcriptome is the complete set and quality of transcripts in a cell. In mammals, host immune response to IAVs have been well elucidated through mRNA and microRNA transcriptomic analyses using hybridization-based approach (microarray) and/or deep sequencing (RNA-Seq) technologies (Baskin *et al*. 2009; Buggele *et al*. 2012; Shoemaker *et al*. 2015). Recently, transcriptomic and functional analyses indicated that IFITM123 (interferon-induced transmembrane protein 1–3) and RIG-I play a crucial role in ducks' tolerance to AIs (Barber *et al*. 2010; Smith *et al*. 2015). However, duck immune response to IAVs is still poorly understood. We previously drew the draft of the duck genome and performed deep lung mRNA transcriptomic analyses of ducks infected by H5N1 viruses (Huang *et al*. 2013). These works opened the window to illuminate ducks' immune response to AIs.

In this article, we compared pathogenicity of two H5N1 virus strains in ducks. We generated 14 mRNA novel transcriptomes of brains and spleens from control ducks and ones that were infected by either a highly pathogenic DK/49 or a weakly pathogenic GS/65 H5N1 virus. We then detected significant differential expressed genes (DEGs) and compared alternative isoform profiles in two H5N1 virus infection against control ducks and the highly pathogenic H5N1 (DK/49) infection against the weakly pathogenic H5N1 (GS/65) infection. Moreover, we identified co-expressional modules highly correlated with virus titers by the WGCNA analysis. We further identified new anti-viral genes and demonstrated that they executed efficiently antiviral activity against both the highly pathogenic and weakly pathogenic H5N1 viruses.

2. Materials and methods

2.1. Facility

Studies of the H5N1 viruses (the DK/49 and GS/65) were conducted in a biosecurity level 3+ laboratory approved by the Ministry of Agriculture and Rural Affairs of China. All animal studies were approved by the Review Board of Harbin Veterinary Research Institute, Chinese Academy of Agricultural Sciences. The study was performed in strict accordance with the recommendation in the Guide for the Care and Use of Laboratory Animals. Protocols for the animal studies were approved by the Committee on the Ethics of the Animal Experiments of the Harbin Veterinary Research Institute, Chinese Academy of Agricultural Sciences.

2.2. Duck infection

Samples of H5N1 virus infection and control ducks were collected in our previous study (Huang *et al*. 2013). In brief, the DK/49 and GS/65 H5N1 viruses isolated from a duck and a goose during the avian influenza outbreak of 2005 in China were propagated in 10-day-old fertilized chicken eggs. Two groups of 4-week-old SPF (specific pathogen-free) Shaoxing ducks from the Harbin Veterinary Research Institute, China Academy of Agricultural Science, were inoculated intranasally with 10^3 of 50% egg infectious doses (EID_{50}) of the DK/49 and GS/65 viruses after adapted to a biosecurity level 3+ environment for four days. Brain, spleen, lung, tracheas and duodenum tissues were collected from the above H5N1 virus-infected ducks on day 1, 2 and 3 after inoculation and from uninfected 4-week-old SPF ducks (n=3). Approximately 100 mg of each brain, spleen and lung tissue were used to extract total RNA. Brain, spleen, tracheas and duodenum tissues were detected by virus isolation in 10-day-old chicken embryos as previously described (Song *et al*. 2011). Positive samples were subjected to virus titer determination by calculating the EID_{50} individually using the Reed and Muench method (Reed and Muench 1938). Virus-containing culture supernatant was collected at various time points (hour post-infection) and titrated in eggs. The growth data shown are the average results of three independent experiments.

2.3. Transcriptomic analyses

cDNA libraries of brain and spleen tissues were prepared

according to the manufacturer's instruction (Illumina, San Diego, California, USA) and sequenced on the Illumina Genome Analyzer using the same methods as our previous study. Gene expression was detected using the same methods described in our previous study (Huang *et al*. 2013). Alternative splicing events were detected using the PASA pipeline (Haas *et al*. 2003). The pipeline started with a special sequence cleaning utility, where polyadenylation was identified and stripped. Mapping was performed using BLAT and perfectly mapped reads were selected. Splicing sites at inferred intron boundaries (donor and acceptor sites) supported by consensus mapped reads were clustered and assembled into special gene structures called assemblies. These assemblies were merged if they have the same genomic loci or 95% overlap. The result was classified in four different events (exon skipping, ES; intron retention, IR; alternative 5′ splice site, A5SS; alternative 3′ splice site, A3SS).

2.4. Data availability

Duck transcript sequencing data have been deposited under GenBank Gene Expression Omnibus (GEO) accession PRJNA273367 (BioProject) and Short Read Archieve (SRA) accession SRP052742.

2.5. Gene co-expressional analyses

Co-expression networks were built using the WGCNA package (Langfelder and Horvath 2008). First, the absolute value of the Pearson correlation coefficient was computed for all pairs of molecules. We then choose a power using the scale-free topology criterion. After that, we constructed networks using the blockwiseModules function in the WGCNA package with the minimum module size to 50 genes, and the minimum height for merging modules at 0.25. For each module, we calculated module membership (also known as module eigengene based connectivity k_{ME}) based on Pearson's correlation (Langfelder and Horvath 2008). We ranked modules to define top connections by k_i (connection strength) after filtering with module eigengene based connectivity (k_{ME}≥0.90), gene significance to virus titer of four tissues (the maximum absolute of GS value≥0.80) and change of gene expression (the maximum fold change≥3.0 and FDR≤0.001). To visualize the modules, the 550 top connections were drawn using the Path designer of the IPA (http://www.ingenuity.com/).

2.6. Generation of DF1 cells over-expressing duck gene

The full-length cDNAs of *RIG-I*, *MX1*, *BCL2L15* and *DCSTAMP* were amplified from the lung tissue of the DK/49-infected duck on day 1 after inoculation by PCR reaction using primers listed in Appendix D. These PCR productions were cloned into the PiggyBac expression vector (SBI, Mountain View, CA) at *Mlu*I and *Pme*I sites to generate recombinant plasmid, which contained carboxy-terminal FLAG tag. After that, DF1 cells culturing in DMEM with 10% FBS were transfected with recombinant plasmid using the lipid-based reagent Fugene HD (Program, Madison, USA).

2.7. Quantitative RT-PCR

cDNA was generated from total RNA using the ImProm-II™ Reverse Transcriptase (Promega, Madison, USA) according to the manufacturer's instructions. Expression of 18 chicken genes were estimated by quantitative RT-PCR on the ABI Prism® 7500 (ABI, California, USA) using loci-specific primers (Appendix D) and SYBR Green Master PCR Mix (ABI). We choose the *GAPDH* as a housing keep gene, which shows a relatively constant expression and translation in lung, spleen and brain of ducks and DF1 cells after infected by the DK/49 or GS/65 viruses. The expression of chicken genes was normalized to that of *GAPDH*.

3. Results

3.1. Global gene expression pattern in the highly pathogenic and weakly pathogenic H5N1 virus infection

We found that ducks inoculated with the DK/49 virus showed dramatic disease symptom and seemed to lose weight after inoculation on day one to three: nine died within three days and two developed severe neurological dysfunction (such as ataxia and torticollis) on day two. In contrast, the GS/65-infected ducks showed a mild disease sign, regained energy and started gaining weight on day three: no acute neurological symptom or death within three days (Appendix A). Detailed analyses indicated that the DK/49-infected ducks had a higher virus titer in brain, trachea, lung and duodenum than the corresponding in the GS/65-infected ducks on day one, but they showed similar level of virus titer in these tissues on day 2 and 3 (Fig. 1-A; Appendix B).

We examined global gene profiles of these individuals through transcriptomic analyses (see Section 2). In brain, alignment of approximately 910 million Illumina 90-bp paired-end reads with the merged reference gene set consisting of 20 647 protein-coding genes showed that the DK/49 infection had 18 019 to 18 125 expressed genes, and the GS/65 infection had 17 599 to 18 060 expressed genes (Table 1). In spleen, transcriptomic analyses with approximate 945 million Illumina 90-bp paired-end reads showed that DK/49

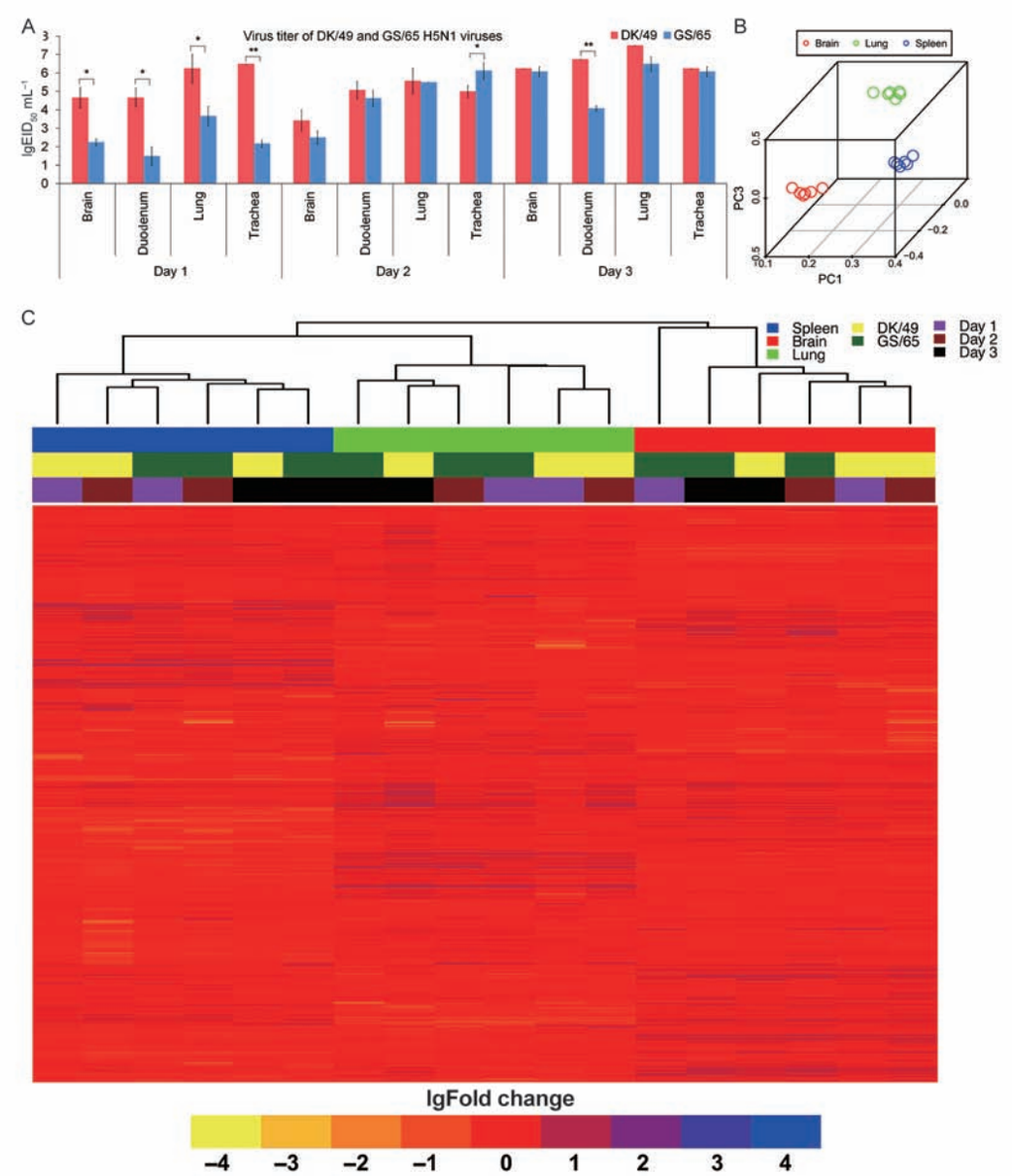

Fig. 1 Virus titers and mRNA profiles of ducks infected with H5N1 viruses. Genes or miRNAs included here described in at least one experiment. A, viral titers and shedding of the DK/49 and GS/65 H5N1 viruses in ducks. Data shown are the mean±standard deviation. *, $P \leq 0.05$; **, $P \leq 0.01$. B, 3D scatter plots of the first three principal component analysis (PCA) based on expressions of 20 051 genes. The proportion of explained variation is annotated on each axis. C, gene profiles in the DK/49- or GS/65-infected ducks and control animals. The heatmap was generated from hierarchical cluster analyses of both genes and samples. Hierarchical clusters of genes and samples were based on Pearson's correlation and Spearman's rank correlation analyses, respectively. Genes shown blue had upregulated expression, and those shown in yellow had downregulated expression in infected ducks relative to controls.

infection had 16 978 to 17 330 described genes, and the GS/65 infection had 17 251 to 17 327 described genes. These observations suggested that the DK/49 infection had similar number of expressed genes to the corresponding of the GS/65 infection in brain and spleen, as well as in lung (Table 1) (Huang *et al*. 2013). After collecting 7 transcriptomes from brain, spleen and lung, we detected a total of 20 051 genes transcribed in control ducks and one infected by either the DK/49 or the GS/65 virus (Huang *et al*. 2013). We performed principal component analysis (PCA) through k-means clustering using gene expression values (reads of per kilo bases per million reads, RPKM) of seven brain, spleen and lung transcriptomes. According to the three eigenvectors of the PCA, samples clustered

dependent on tissue, while independent on virus strain and day after inoculation (Fig. 1-B). This expressional pattern was further supported by the hierarchical clustering analyses, which showed the transcriptomic dendrogram of 21 transcriptomes was divided into three distinct branches representing brain, spleen and lung tissues (Fig. 1-C).

3.2. Changes in gene profiles are more numerous in the highly pathogenic H5N1 infection than the weakly pathogenic H5N1 virus infection

We detected genes showing significantly differential expression in the DK/49 infection or the GS/65 infection against control ducks, as well as between these two H5N1 virus infection using the thresholds of FDR≤0.001 and fold change≥2. This effort found that the DK/49-infected ducks had a merged DEGs set with larger number DEGs in brain (DEG set 1: 3 879 DEGs) and spleen (DEG set 3: 5 501 DEGs) than the GS/65-infected ducks did (DEG set 2 in brain: 2 427 DEGs; DEG set 4 in spleen: 3 537 DEGs). Combined with previous seven lung transcriptomes, we totally detected 9 350 DEGs in the DK/49 infection and 6 156 DEGs in the GS/65 infection. We also detected a merged DEG set with large number DEGs in brain (DEG set 5: 3 773 DEGs) and spleen (DEG set 6: 3 551 DEGs) in the DK/49-infected ducks when compared to the GS/65-infected ducks (Table 1). Among these DEGs in brain, 451 and 152 genes changed their expressions significantly in all DK/49-infected ducks and GS/65-infected ducks respectively, while 103 genes changed their expression remarked between DK/49-infected ducks and GS/65-infected ducks on all day 1 to 3 after inoculation (Appendix E). In spleens, 648 and 664 genes continuously changed their expressions significantly in all DK/49-infected ducks and GS/65-infected ducks respectively, while 97 genes continuously changed their expression remarked between DK/49-infected ducks and GS/65-infected ducks on day one to three after inoculation (Appendix E). We then performed functional categories of these six DEG sets with the Ingenuity Pathway Analysis (IPA). IPA of DEG set one–four identified six enriched categories (cellular development, cell-to-cell signaling and interaction, cellular development, cell growth and proliferation, cellular function and maintenance, and cell signaling) were related to cell activation (P≤0.001, Appendix F) (http://www.ingenuity.com/). IPA analyses also showed that one enriched category related to lipid metabolism and one enriched category related to molecular transport were identified in DEG set two–four (Appendix F). Furthermore, IPA analysis of DEG set five and six identified one enriched category related to lipid metabolism, one enriched category related to molecular transport categories, and four enriched categories related to cell activation (cellular movement, cell-to-cell signaling and interaction, cell development and cell signaling).

After that, we used 177 immune genes, which included

Table 1 Information of mRNA profiles in control and H5N1 virus-infected ducks

Tissues	Group	Total reads	Total length of reads (bp)	Number of uniquely mapped reads		Number of expressed genes	Number of DEGs (*vs.* control)[1)]		Number of DEGs (*vs.* GS/65-infected ducks)[1)]	
				Genome	Gene		DEGs	DEG set	DEGs	DEG set
Brain	Control	131 405 156	11 826 464 040	71 748 108	50 357 585	18 095				
	DK/49 (day 1)	160 913 400	14 482 206 000	88 863 619	61 392 964	18 125	942		1 938	
	DK/49 (day 2)	132 679 178	11 941 126 020	73 038 160	52 436 094	18 019	1 239		606	
	DK/49 (day 3)	123 828 950	11 144 605 500	71 828 269	51 649 871	18 097	3 336	3 878	2323	3 773
	GS/65 (day 1)	122 182 596	10 996 433 640	64 087 263	46 232 742	17 599	811			
	GS/65 (day 2)	100 993 320	9 089 398 800	56 487 260	39 554 868	17 909	1365			
	GS/65 (day 3)	137 535 354	12 378 181 860	77 354 065	54 545 647	18 060	1 199	2 427		
Spleen	Control	121 768 450	10 959 160 500	65 936 715	57 005 523	17 625				
	DK/49 (day 1)	138 676 330	12 480 869 700	72 722 480	60 619 485	17 330	1 168		763	
	DK/49 (day 2)	137 893 486	12 410 413 740	72 677 936	62 902 782	17 027	4 343		2 574	
	DK/49 (day 3)	134 970 442	12 147 339 780	72 066 279	64 317 428	16 978	3 019	5 501	1 042	3 551
	GS/65 (day 1)	142 462 174	12 821 595 660	76 447 588	67 025 450	17 327	1 505			
	GS/65 (day 2)	129 507 204	11 655 648 360	70 214 136	61 715 613	17 281	2 096			
	GS/65 (day 3)	139 671 228	12 570 410 520	71 675 969	60 223 762	17 251	2 149	3 537		

[1)]DEGs are genes that showed significantly different expression with FDR≤0.001 and fold change≥2.

three RNA helicases, four T cell receptors, five colony stimulating factors, five interferon-induced proteins, ten toll-like receptors, and 150 cytokines annotated in our previous study (Huang *et al*. 2013), as an example to compare the changes in gene expression in the DK/49 and GS/65 infection against control individuals, and between these H5N1 virus infection. Transcriptomic analyses showed that, the DK/49 infection had a total of 88 and 111 immune genes significantly changed their expression (FDR≤0.001 and fold change≥2) in brains and spleens respectively (Fig. 2-A, full names are given in Appendix G). In contrast, the GS/65 infection had small numbers of immune genes changing their expression significantly in brains (70 DGEs) and spleens (72 DEGs) (Fig. 2-B). Moreover, we found that 77 and 83 of these 177 duck immune genes showed significantly differential expression in brain and spleen of the DK/49 infection when compared to the corresponding in the GS/65 infection (Fig. 2-C). These observations suggested that highly pathogenic H5N1 viruses might activate more immune genes dramatically and broadly than weakly pathogenic H5N1 viruses did.

3.3. The highly pathogenic and weakly pathogenic H5N1 viruses prefer to affect alternative translation of immune genes

We examined four types of alternative splicing events (SE, IR, A5SS and A3SS), by searching against known and putative splicing junctions using the SOAPsplice software (Appendix H). Alignment of the above ~2 771 million Illumina paired-end reads with the duck genome assembly (BGI_duck_1.0) suggested that totally 136 451 alternative

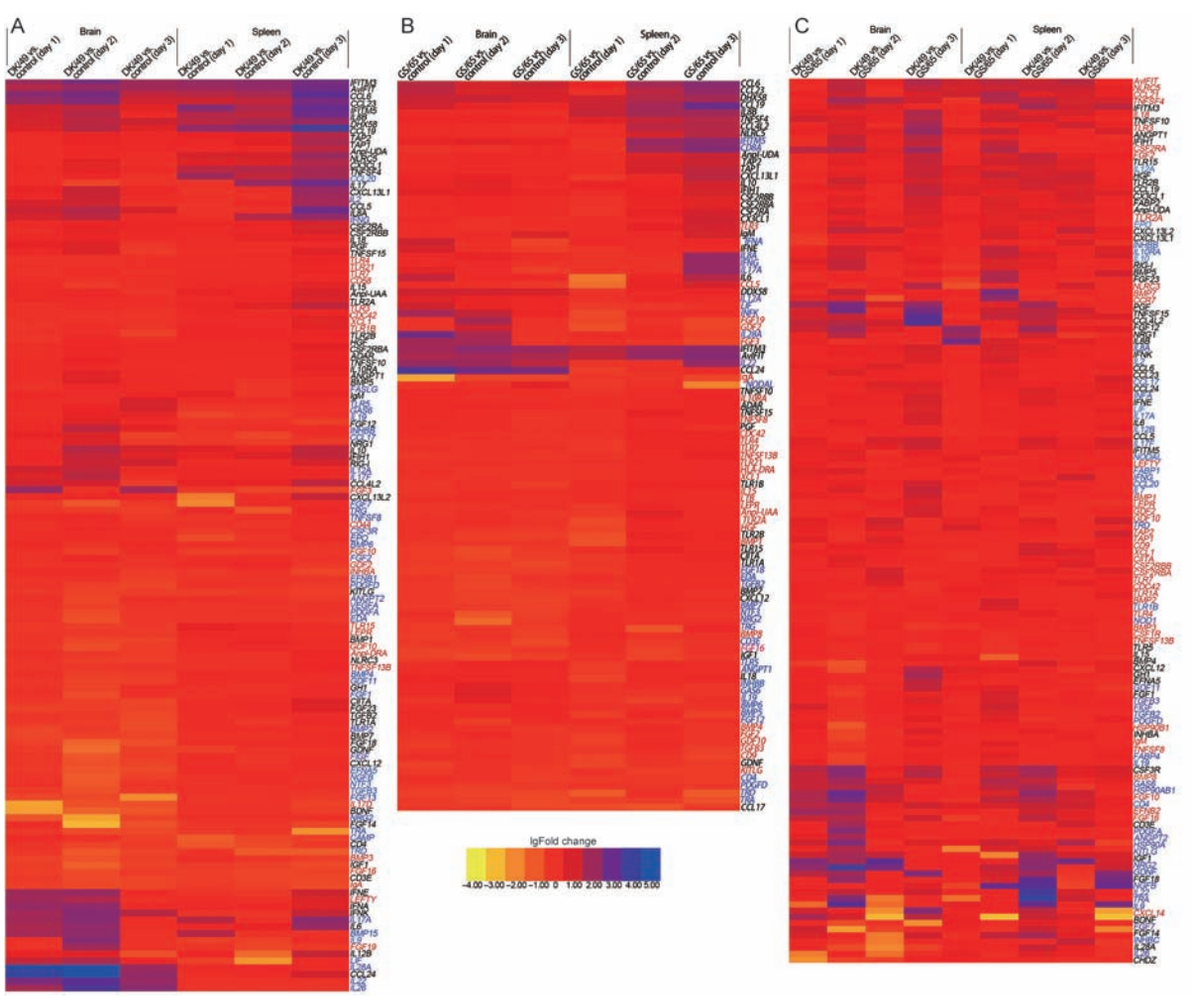

Fig. 2 Identification of genes responsive to H5N1 viruses in ducks. Genes included here showed significant differences in gene expression (FDR≤0.001, fold change≥2) in at least one experiment. The heat map was generated from hierarchical analysis of genes based on Pearson's correlation analyses. A, expression of 134 immune genes in brain and spleen tissues of the DK/49-infected ducks. B, expression of 102 immune genes in brain and spleen tissues of the GS/65-infected ducks. C, expression of 130 immune genes in brain and spleen tissues of the DK/49- or GS/65-infected ducks.

splicing events, which comprised 64.79% expressed genes (12 657), were detected in ducks (Appendix I). Detailed analyses demonstrated that there were 45.12, 51.77 and 55.16% genes expressed alternative splicing events in brain, spleen and lung tissues, respectively (Table 1; Appendices I and J).

To detect novel alternative isoform induced by IAVs, we compared alternative splicing diversity in the DK/49-infected ducks, GS/65-infected ducks and control animals. Firstly, we counted two H5N1 virus-induced splicing events (H5N1ISEs), which alternative splicing events expressed in all infected ducks but not in control animals. This effort identified 350 H5N1ISEs expressed of 283 genes, 566 H5N1IS events of 432 genes and 739 H5N1ISEs of 516 genes in brain, spleen and lung, respectively (Appendix J). Interestingly, 182 of 283 genes, 293 of 432 genes, and 366 of 516 genes showing H5N1ISEs in brain, spleen and lung tissues, respectively, were included in the 9 162 duck immune genes (Appendix C). Detailed analyses of these genes expressed H5N1ISEs suggested that, in brains, 7 genes (*IRF7*, *MX1*, *MITD1*, *PLAC88*, *RNF213*, *TRIM25* and *USP18*) playing critical role in immune response to IAVs, had significantly different expression levels in all H5N1 virus-infected ducks. In spleen, 40 including seven genes (*CCL19*, *RIG-I*, *DDX60*, *DRAM1*, *MDA5*, *MX1* and *VIPERIN*) involved in immune response to IAVs, showed remarkable different expression levels in all DK/49- and GS/65-infected ducks. While in lung, 55 including 9 genes (*ADAR*, *RIG-I*, *DDX60*, *MDA5*, *MX1*, *NLRC5*, *STAT1*, *TRIM25* and *VIPERIN*) involved in immune response to IAVs, changed their expression levels in all DK/49- and GS/65-infected ducks (Fig. 3-A).

We then counted the DK/49 and GS/65 virus strain-specific splicing events (DK/49ISEs and GS/65ISEs), which alternative splicing events expressed in all ducks infected by either the DK/49 or GS/65 virus, but not in control animals and ducks infected with the other strain of H5N1 virus. We totally identified 439 DK/49ISEs of 384 genes, 164 DK/49ISEs of 148 genes and 329 DK/49ISEs of 299 genes in brain, spleen and lung tissues respectively (Appendix J). Among them, 224 of 384 genes, 114 of 148 genes and 205 of 299 genes expressing 49ISEs were in the 9 162 duck immune genes. Detailed analyses suggested that 17 of 384 genes in brain, 5 of 148 genes in spleen, and 24 of 299 genes in lung significantly changed their expression levels in all the DK/49-infected ducks when compared to both control animals and the GS/65-infected ducks (Fig. 3-B). Similarly, we detected 54 GS/65ISEs of 50 genes, 161 GS/65ISEs of 156 genes and 153 GS/65ISEs of 142 genes in brain, spleen and lung tissues respectively (Fig. 3-B). Expectedly, large proportions of genes expressing GS/65ISEs in brain (33 of 50), spleen (98 of 156) and lung (92 of 142) tissues were listed in our defined 9 162 duck immune genes. Further transcriptomic analyses indicated that one of the above 142 genes (*SRGN*) in lung and two of the above 156 genes (*RIG-I* and *ZNFX1*) in spleen had different expressional pattern in all the GS/65-infected ducks when compared to both control animals and the DK/49-infected ducks (Fig. 3-B).

3.4. WGCNA networks response to H5N1 virus infection

We constructed DEG networks of the brain, spleen and lung transcriptomes using the WGCNA analysis (Langfelder and Horvath 2008). Of the total, 4 540 genes in the brain, 5 475 genes in the lung and 6 103 genes in the spleen DEG set were assigned to seven, eleven and fourteen co-expression modules, respectively. The different modules were color-coded for presentation purposes and referred to hereafter using these colors (Fig. 4-A). We determined module significance by correlating gene profile to virus titer in trachea, lung, brain and duodenum using stringent thresholds ($r \geq 0.70$ or $r \leq -0.70$, $P \leq 0.05$). This effort found that no module constructed with the spleen DEG set showed virus titer significance, while five modules from the brain or lung DEG set showed virus titer significance (Fig. 4-B). In brains, all the blue, brown and turquoise modules were highly correlated with virus titer of duodenum. Moreover, the brown module was highly correlated with virus titer of trachea, and the turquoise module was highly correlated with virus titer of lung (Fig. 4-B). Detailed analyses indicated that more than 54% of genes in blue, brown and turquiouse modules were contained in the 9 162 duck immune genes. Interestingly, immune genes in the top 550 connections of the brain turquoise module had a proportion of 70%. Among them, 14 genes (*CASP1*, *CCL21*, *CD40*, *CYBB*, *C1QA*, *RIG-I*, *FAS*, *IRF1*, *PML*, *PTGS2*, *SOCS1*, *STAT1*, *STAT3* and *TAP2*) were known to be involved in immune response to IAVs (Fig. 4-C). In lung, the brown module was highly correlated with virus titer of duodenum. The pink module was highly correlated with virus titer of trachea, lung and duodenum, respectively. Similarly, we found that the brown (61%) and pink (70%) modules had a large proportion of genes listed in the 9 162 duck immune genes. Among them, two (*CSF2Rβ* and *TRIM25*) and seven (*A2M*, *CCR2*, *CD274*, *CXCL13L2*, *RIG-I*, *MX1* and *TLR4*) of the top connections in the pink and brown modules respectively, were implicated to immune response to AIVs (Gack *et al*. 2007; Schneider *et al*. 2014).

3.5. New immune genes responsive to H5N1 virus infection

Comparing molecules of top 550 connections from five

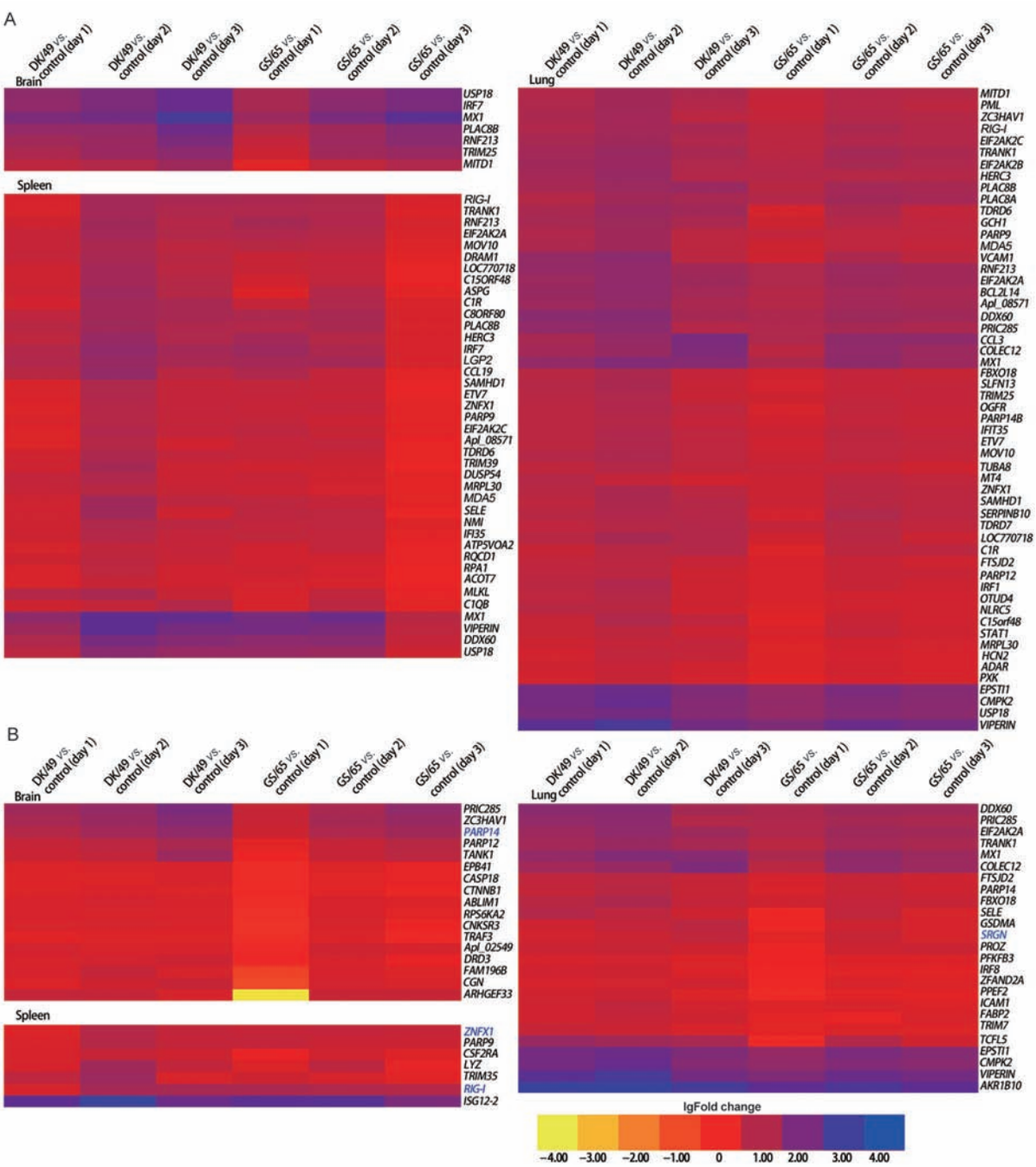

Fig. 3 Profiles of genes having putative alternative splicing events response to H5N1 viruses in ducks. These heatmaps were generated from hierarchical analysis of genes. These 71 genes in A had same alternative splicing events induced by either the DK/49 or GS/65 virus and had significant differential expression in brain, spleen and lung tissues of all the DK/49- and GS/65-infected ducks compared to control animals. These 47 genes in B had the DK/49 or GS/65 virus strain-specific alternative splicing events and significantly altered their genes expression in brain, spleen and lung tissues of all the DK/49- or GS/65-infected ducks compared to control animals, as well as between the DK/49- and GS/65-infected ducks.

modules in the brain or lung DEG set showing virus titers significance, we found that 12 molecules were expressed both in the brain turquoise and lung brown module (Fig. 4-C). Of these 12 molecules, one (*RIG-I*) is a RNA sensor of IAVs (Barber *et al*. 2010; Rehwinkel *et al*. 2010). We further randomly examined profiles of 18 genes in top 550 connections of these two modules and found 11 of them (*BATF3*, *BCL2L14*, *BCL2L15*, *CCR2*, *CD83*, *CD274*, *C8ORF80*, *LY96*, *MARCO*, *MX1* and *TDRD7*) also showed significantly differential expression in DF1 cells (chicken

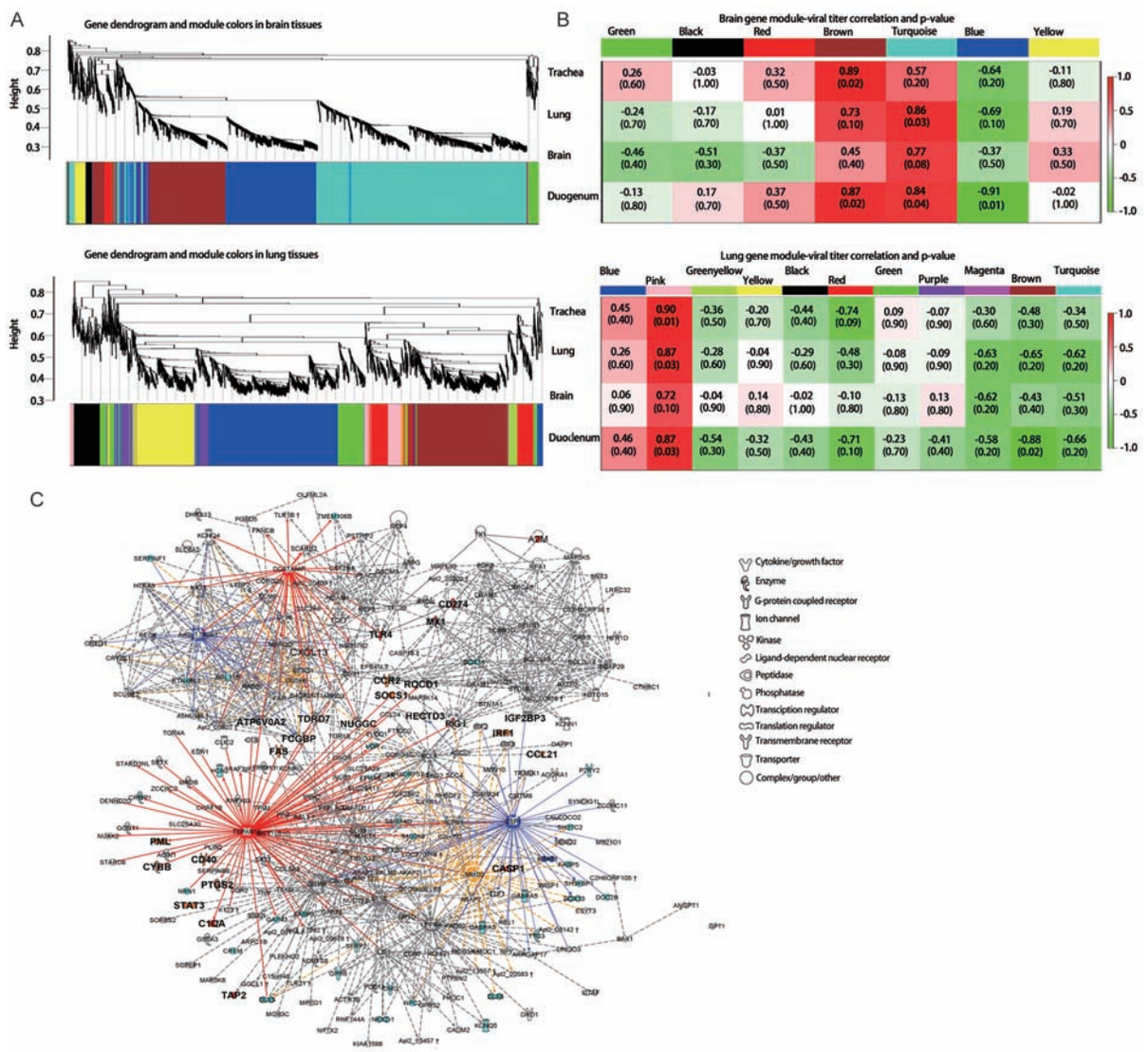

Fig. 4 Gene co-expressional modules associated with immune response to H5N1 viruses. A, hierarchical clustering dendrogram and module definition about the genes in brain and lung. Genes included here showed significant differences in gene expression (FDR≤0.001, fold change≥2) at least one experiment. The dendrogram results were clustered from average linkage hierarchical clustering. The color-band below the dendrogram represents the modules. B, relationships between modules and viral tilters of trachea, lung, brain and duodenum in the brain and lung. Relationships between modules and viral titers were calculated using Pearson's correlation analyses with the WGCNA package (Langfelder *et al*. 2008). Values on the first line and second line in each module are *r*-value and *P*-value, respectively. C, visualization of the top 550 connections in the brain turquoise and the lung brown module. Connections of three genes and their interactors showed in red, orange and blue, respectively. Genes involving into immune response to avian influenza viruses were in bold fonts and red backgrounds, and these were also involving into neuronal activity were in bold fonts and orange backgrounds. Genes involving neuronal activity were in cyan backgrounds.

embryonic fibroblasts) at 48 h after inoculated by the DK/49 virus (Appendix K). This observation encouraged us to further investigate biological functions of molecules in these two modules. We constructed recombinant plasmids of four molecules including two (*RIG-I* and *MX1*) known as important immune genes to IAVs and the other two genes (*BCL2L15* and *DCSTAMP*) in the lung brown module (Figs. 4-C and 5-A). We calculated virus titer of DF1 cells transfected with one of four recombinant plasmids or plasmid only (mock cells) after inoculated by either the DK/49 or GS/65 virus at six time points (post infection at 12, 24, 36, 48, 60 and 72 h). This calculation suggested that DF1 cells expressing duck *RIG-I* exhibited lower level (P≤0.05) replication of both the DK/49 (at 24, 36, 48 and 60 h) and GS/65 (at 36, 60 and 72 h) virus than mock cells did. Similarly, DF1 cells expressing duck *MX1* had lower level (P≤0.05) replication of both the DK/49 (at 24, 36, 48 and 60 h) or GS/65 (at 12, 36, 48, 60 and 72 h) virus than

mock cells did (Fig. 5-B). Interestingly, markedly reduced replication of both the DK/49 and GS/65 viruses ($P \leq 0.05$) was observed in DF1 cells transfected with either the duck *BCL2L15* or *DCSTAMP* (Fig. 5-B).

4. Discussion

H5N1 AIs, causing an acute viral disease of the respiratory tract in birds and even association with lethal human infection, have raised significant global health concern. Many fundamental discoveries for resistance and counter-resistance between hosts and H5N1 viruses had been made. For example, it was reported that H5N1 virus infection caused severe pneumonia and increased expression of neutrophil chemoattractant in rhesus macaque, and activated signaling pathways related to specific imbalanced inflammatory response in human endothelial cells (Shinya *et al*. 2012). In chicken, H5N1 virus infection induced excessive expression of IFNs, cytokines and ISGs (Ranaware *et al*. 2016). Here our data for systemic gene profiles of highly or weakly pathogenic H5N1 virus infection and control animal, in combination with interactional analysis among genes and viruses, recapitulated an active fight between IAVs and ducks. In one hand, both the highly and the weakly pathogenic H5N1 virus infection led to significantly differential expression of many innate immune genes, for example, three RNA helicases, four T cell receptors, five colony stimulating factors, ten toll-like receptors and more than 109 cytokines (Fig. 2-C). Such remarked change in expression of innate immune genes induced an antiviral state and instructed the adaptive immune response to IAVs, even successfully removed IAVs *in vivo* (Iwasaki and Pillai 2014). Our observation in pathogenicity of H5N1 virus on ducks together with previous studies showed the GS/65-infected ducks appeared healthy within three days after infection, implying that the duck's immune system had the advantage in the fight to this weakly pathogenic H5N1 virus. However, the duck's immune system seemed to be evaded by the highly pathogenic H5N1 virus, where the DK/49-infected ducks showed severe neurological sign and died within four days after infection (Song *et al*. 2011). Such difference in the virulence of these two H5N1 viruses in ducks might partly be attributed to the highly pathogenic H5N1 virus caused more serious dysregulation of the

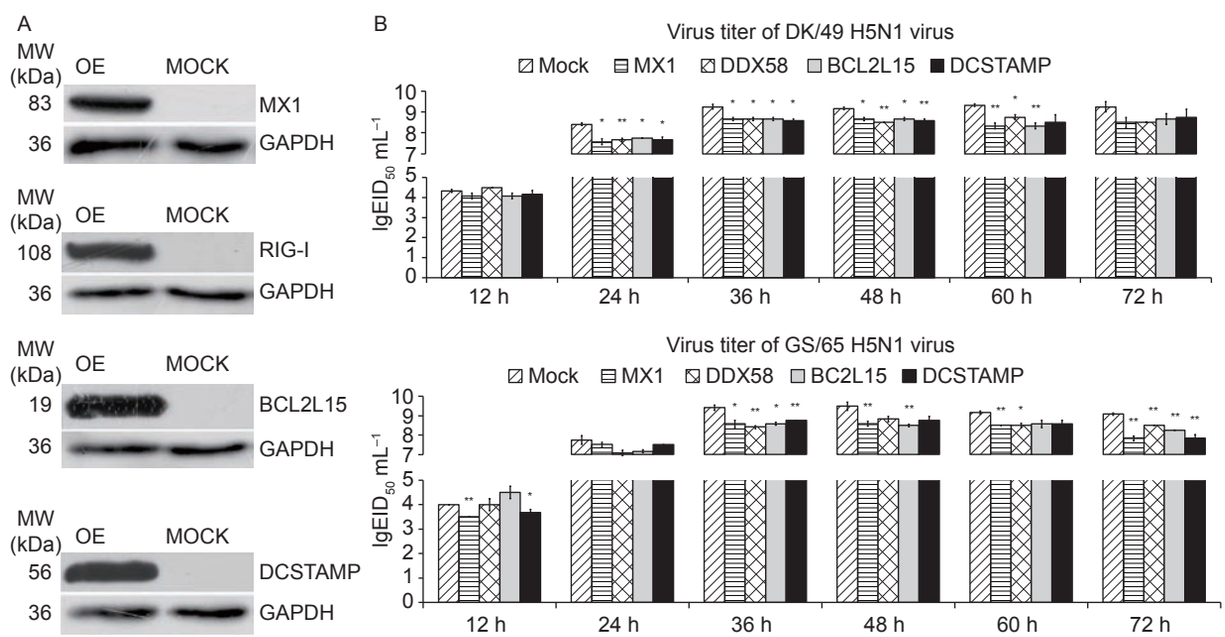

Fig. 5 Duck RIG-I, MX1, BCL2L15 and DCSTAMP proteins reduce H5N1 viruses' replication in DF1 cells. Mock, RIG-I, MX1, BCL2L15 and DCSTAMP mean that DF1 cells transfected plasmid, recombinant plasmids expressing either duck RIG-I, MX1, BCL2L15 or DCSTAMP respectively. A, protein expression of four duck genes in DF1 cells. The RIG-I, MX1, BCL2L15 and DCSTAMP proteins were detected from total cell lysates with anti-FLAG antibody through the Western blot analyses. OE and MOCK represent DF1 cells transfected recombinant plasmid or empty plasmid, respectively. Cropped blots are displayed. Representative images are presented and full-length Western blots are presented in Appendix L. GAPDH served as control in the western blot analysis. B, multicycle replication of two H5N1 viruses in DF1 cells. DF1 cells were inoculated at multiplicity of infection (MOI) of 0.001 with either the DK/49 or GS/65 virus, and the culture supernatants of DF1 cells were collected at the indicated hour post-infection (hpi) and then titrated in eggs (two-tailed Student's test, n=3). The data are expressed as the mean±SD. *, P<0.05; **, P<0.01.

antiviral response than the weakly pathogenic H5N1 virus did. For example, when compared to the weakly pathogenic H5N1 virus-infected ducks, two RNA helicases (RIG-I and MDA5) were continuously increased by 1.27- to 3.75-fold in all brain, spleen and lung, except in spleen on day one and brain on day two, of the highly pathogenic H5N1 virus-infected ducks. The increasing expression of two RNA helicases (RIG-I and MDA5) and their binding to IAVs, in return increase their pathways, which led to excessive elevation of IFNs (i.e., *IFNA* by 175-fold, *IFNE* by 102-fold and *IFNG* by 21-fold) and cytokines (i.e., *IL6* by 118-fold, *IL28A* by 1 110-fold and *IL22* by 26-fold) (Fig. 2-C and Appendix M). This is similar to the case in chicken, where H5N1 virus infection but not H9N2 virus infection induced excessive expression of *IFNA*, *IFTM3*, *TGFB3*, *IL12B*, *IL13* and *IL17F* (Ranaware *et al*. 2016).

IAVs have evolved to evade or subvert the innate immune response through interfering splicing of cellular genes. Alternative splicing of some genes involved into immune response to influenza A virus may interfere with their antiviral activity. For example, one truncated variant of MAVS interferes with interferon production induced by full-length MAVS and a variant MX1 isoform induced by herpes simplex virus-1 enhances viral replication (Ku *et al*. 2011; Brubaker *et al*. 2014). Comparing transcriptomic diversity in H5N1 virus infection and control duck, we found that both the highly and weakly pathogenic H5N1 viruses induced 1 578 new alternative splicing events in 1 092 genes. Among them, 745 genes were listed in 9 162 duck immune genes, and 71 including 12 (*ADAR*, *CCL19*, *RIG-I*, *DDX60*, *LGP2*, *MDA5*, *IRF7*, *MX1*, *NLRC5*, *STAT1*, *TRIM25* and *VIPERIN*) genes playing critical role in immune response to IAVs, changed their expression significantly in brain, spleen or lung of all H5N1 virus infection. This observation implied that IAVs might induce new isoforms of immune genes to suppress duck's immune systems and enhance of IAVs' replication; therefore, a functional analysis of new isoforms of immune genes induced by IAVs (i.e., *RIG-I* and *MDA5*) in birds will be interesting.

Although mice *MX1* plays important role in resistance to IAVs through blocking their primary transcription and clearing viruses rapidly, avian MX1's role in immune response to IAVs is controversial for long time (Bazzigher *et al*. 1993; Ko *et al*. 2002; Verhelst *et al*. 2015; Pillai *et al*. 2016). Here we found that duck *MX1* in top 550 connection of lung brown module and confirmed its antiviral activity to AIVs. Moreover, we took two highly connected genes (*BCL2L15* and *DCSTAMP*) together with one immune gene (*RIG-I*) from the top 550 connections in the lung brown module as examples to test their antiviral activity to AIVs. Interestingly, our data showed that both two genes (*BCL2L15* and *DCSTAMP*) and *MX1* significantly reduced both the highly and weakly pathogenic H5N1 virus replication in DF1 cells, like the duck *RIG-I* did (Fig. 5-B). For these two genes, *BCL2L15* is a novel proapoptotic member of the BCL2 protein family and weakly promoted apoptosis and antagonized BCL2's prosurvival function (Pujianto *et al*. 2007). *DCSTAMP* is a novel dendritic cells (DCs) specific multimembrane spanning protein that has been implicated in skewing haematopoietic differentiation of bone marrow cells (Yagi *et al*. 2005; Jansen *et al*. 2009). This study, in our knowledges, demonstrated for the first time that *BCL2L15* and *DCSTAMP* were implicated to immune response to viruses.

5. Conclusion

Our results suggested that, like in human, correlation trait variation with duck's co-expressional network analysis provided a list of genes and networks these likely played important roles in H5N1 virus infection. Hopefully, this work will provide a foundation to understand interaction between host and IAVs. Future, integration of molecular data using genetic manipulations with our systems-level networks has the potential to reveal a more detailed picture of the particular molecular features depicted in the network that contribute to host immune response to IAVs.

Acknowledgements

We would like to thank Mr. Zou Shijie from BGI-Shenzhen, China, Dr. Liu Tongxin and Dr. Yang Zhi from China Agricultural University for RNA purification assistance. The sequencing of the duck transcriptomes was funded by the National Natural Science Foundation of China (31471176) and the Fundamental Research Funds for the Central Universities, China (15054034).

Appendices associated with this paper can be available on http://www.ChinaAgriSci.com/V2/En/appendix.htm

References

Barber M R, Aldridge Jr J R, Webster R G, Magor K E. 2010. Association of RIG-I with innate immunity of ducks to influenza. *Proceedings of the National Academy of Sciences of the United States of America*, **107**, 5913–5918.

Baskin C R, Bielefeldt-Ohmann H, Tumpey T M, Sabourin P J, Long J P, Garcia-Sastre A, Tolnay A E, Albrecht R, Pyles J A, Olson P H, Aicher L D, Rosenzweig E R, Murali-Krishna K, Clark E A, Kotur M S, Fornek J L, Proll S, Palermo R E, Sabourin C L, Katze M G. 2009. Early sustained innate immune response defines pathology and death in nonhuman primates infected by highly pathogenic influenza virus. *Proceedings of the National Academy of Sciences of the United States of America*, **106**, 3455–3460.

Bazzigher L, Schwarz A, Staeheli P. 1993. No enhanced influenza-virus resistance of murine and avian cells expressing cloned duck mx protein. *Virology*, **195**, 100–112.

Brubaker S W, Gauthier A E, Mills E W, Ingolia N T, Kagan J C. 2014. A bicistronic MAVS transcript highlights a class of truncated variants in antiviral immunity. *Cell*, **156**, 800–811.

Buggele W A, Johnson K E, Horvath C M. 2012. Influenza A virus infection of human respiratory cells induces primary microRNA expression. *Journal of Biological Chemistry*, **287**, 31027–31040.

Deng G H, Shi J Z, Wang J, Kong H H, Cui P F, Zhang F, Tan D, Suzuki Y, Liu L L, Jiang Y P, Guan Y T, Chen H L. 2015. Genetics, receptor binding, and virulence in mice of H10N8 influenza viruses isolated from ducks and chickens in live poultry markets in China. *Journal of Virology*, **89**, 6506–6510.

Deng G H, Tan D, Shi J Z, Cui P F, Jiang Y P, Liu L L, Tian G B, Kawaoka Y, Li C J, Chen H L. 2013. Complex reassortment of multiple subtypes of avian influenza viruses in domestic ducks at the dongting lake region of China. *Journal of Virology*, **87**, 9452–9462.

Gack M U, Shin Y C, Joo C H, Urano T, Liang C, Sun L J, Takeuchi O, Akira S, Chen Z J, Inoue S S, Jung J U. 2007. TRIM25 RING-finger E3 ubiquitin ligase is essential for RIG-I-mediated antiviral activity. *Nature*, **446**, 916-920.

Gao Y W, Zhang Y, Shinya K, Deng G H, Jiang Y P, Li Z J, Guan Y T, Tian G B, Li Y B, Shi J Z Liu L L, Zeng X Y, Bu Z G, Xia X Z, Kawaoka Y, Chen H L. 2009. Identification of amino acids in HA and PB2 critical for the transmission of H5N1 avian influenza viruses in a mammalian host. *PLoS Pathogens*, **5**, e1000709.

Haas B J, Delcher A L, Mount S M, Wortman J R, Smith R K, Hannick L I, Maiti R, Ronning C M, Rusch D B, Town C D, Salzberg S L, White O. 2003. Improving the *Arabidopsis* genome annotation using maximal transcript alignment assemblies. *Nucleic Acids Research*, **31**, 5654–5666.

Huang Y H, Li Y R, Burt D W, Chen H L, Zhang Y, Qian W B, Kim H, Gan S Q, Zhao Y Q, Li J W, Yi K, Feng H P, Zhu P Y, Li B, Liu Q Y, Fairley S, Magor K E, Du Z L, Hu X X, Goodman L. 2013. The duck genome and transcriptome provide insight into an avian influenza virus reservoir species. *Nature Genetics*, **45**, 776–783.

Inouye M, Silander K, Hamalainen E, Salomaa V, Harald K, Jousilahti P, Mannisto S, Eriksson J G, Saarela J, Ripatti S, Perola M, van Ommen G J B, Taskinen M R, Palotie A, Dermitzakis E T, Peltonen L. 2010. An immune response network associated with blood lipid levels. *PLoS Genetics*, **6**.

Iwasaki A, Pillai P S. 2014. Innate immunity to influenza virus infection. *Nature Reviews Immunology*, **14**, 315–328.

Jansen B J H, Eleveld-Trancikova D, Sanecka A, Van Hout-Kuijer M, Hendriks I A M, Looman M G W, Leusen J H W, Adema G J. 2009. OS9 interacts with DC-STAMP and modulates its intracellular localization in response to TLR ligation. *Molecular Immunology*, **46**, 505–515.

Ko J H, Jin H K, Asano A, Takada A, Ninomiya A, Kida H, Hokiyama H, Ohara M, Tsuzuki M, Nishibori M, Mizutani M, Watanabe T. 2002. Polymorphisms and the differential antiviral activity of the chicken *Mx* gene. *Genome Research*, **12**, 595–601.

Ku C C, Che X B, Reichelt M, Rajamani J, Schaap-Nutt A, Huang K J, Sommer M H, Chen Y S, Chen Y Y, Arvin A M. 2011. Herpes simplex virus-1 induces expression of a novel MxA isoform that enhances viral replication. *Immunology and Cell Biology*, **89**, 173–182.

Langfelder P, Horvath S. 2008. WGCNA: An R package for weighted correlation network analysis. *BMC Bioinformatics*, **9**, 559.

Pillai P S, Molony R D, Martinod K, Dong H, Pang I K, Tal M C, Solis A G, Bielecki P, Mohanty S, Trentalange M, Homer R J, Flavell R A, Wagner D D, Montgomery R R, Shaw A C, Staeheli P, Iwasaki A. 2016. Mx1 reveals innate pathways to antiviral resistance and lethal influenza disease. *Science*, **352**, 463–466.

Pujianto D A, Damdimopoulos A E, Sipila P, Jalkanen J, Huhtaniemi I, Poutanen M. 2007. *Bfk*, a novel member of the *Bcl2* gene family, is highly expressed in principal cells of the mouse epididymis and demonstrates a predominant nuclear localization. *Endocrinology*, **148**, 3196–3204.

Ranaware P B, Mishra A, Vijayakumar P, Gandhale P N, Kumar H, Kulkarni D D, Raut A A. 2016. Genome wide host gene expression analysis in chicken lungs infected with avian influenza viruses. *PLoS ONE*, **11**, e0153671.

Reed L, Muench H. 1938. A simple method of estimating fifty per cent endpoints. *American Journal of Epidemiology*, **27**, 493–497.

Rehwinkel J, Tan C P, Goubau D, Schulz O, Pichlmair A, Bier K, Robb N, Vreede F, Barclay W, Fodor E, Sousa C R E. 2010. RIG-I detects viral genomic RNA during negative-strand RNA virus infection. *Cell*, **140**, 397-408.

Schneider C, Nobs S P, Heer A K, Kurrer M, Klinke G, van Rooijen N, Vogel J, Kopf M. 2014. Alveolar macrophages are essential for protection from respiratory failure and associated morbidity following influenza virus infection. *PLoS Pathogens*, **10**, e1004053.

Shinya K, Gao Y, Cilloniz C, Suzuki Y, Fujie M, Deng G, Zhu Q, Fan S, Makino A, Muramoto Y, Fukuyama S, Tamura D, Noda T, Eisfeld A J, Katze M G, Chen H L, Kawaoka Y. 2012. Integrated clinical, pathologic, virologic, and transcriptomic analysis of H5N1 influenza virus-induced viral pneumonia in the rhesus macaque. *Journal of Virology*, **86**, 6055–6066.

Shoemaker J E, Fukuyama S, Eisfeld A J, Zhao D M, Kawakami E, Sakabe S, Maemura T, Gorai T, Katsura H, Muramoto Y, Watanabe S, Watanabe T, Fuji K, Matsuoka Y, Kitano H, Kawaoka Y. 2015. An ultrasensitive mechanism regulates influenza virus-induced inflammation. *PLoS Pathogens*, **11**, e1004856.

Smith J, Smith N, Yu L, Paton I R, Gutowska M W, Forrest H L, Danner A F, Seiler J P, Digard P, Webster R G, Burt D W. 2015. A comparative analysis of host responses to avian influenza infection in ducks and chickens highlights a role for the interferon-induced transmembrane proteins in viral

resistance. *BMC Genomics*, **16**, 574.

Song J S, Feng H P, Xu J, Zhao D M, Shi J Z, Li Y B, Deng G H, Jiang Y P, Li X Y, Zhu P Y, Guan Y T, Bu Z G, Kawaoka Y, Chen H L. 2011. The PA protein directly contributes to the virulence of H5N1 avian influenza viruses in domestic ducks. *Journal of Virology*, **85**, 2180–2188.

Tong S X, Zhu X Y, Li Y, Shi M, Zhang J, Bourgeois M, Yang H, Chen X F, Recuenco S, Gomez J, Chen L M, Johnson A, Tao Y, Dreyfus C, Yu W L, McBride R, Carney P J, Gilbert A T, Chang J, Guo Z. 2013. New world bats harbor diverse influenza A viruses. *PLoS Pathogens*, **9**, e1003657.

Verhelst J, Spitaels J, Nurnberger C, De Vlieger D, Ysenbaert T, Staeheli P, Fiers W, Saelens X. 2015. Functional comparison of Mx1 from two different mouse species reveals the involvement of loop L4 in the antiviral activity against influenza A viruses. *Journal of Virology*, **89**, 10879–10890.

Voineagu I, Wang X C, Johnston P, Lowe J K, Tian Y, Horvath S, Mill J, Cantor R M, Blencowe B J, Geschwind D H. 2011. Transcriptomic analysis of autistic brain reveals convergent molecular pathology. *Nature*, **474**, 380–384.

Yagi M, Miyamoto T, Sawatani Y, Iwamoto K, Hosogane N, Fujita N, Morita K, Ninomiya K, Suzuki T, Miyamoto K, Oike Y, Takeya M, Toyama Y, Suda T. 2005. DC-STAMP is essential for cell-cell fusion in osteoclasts and foreign body giant cells. *Journal of Experimental Medicine*, **202**, 345–351.

Zhang Y, Zhang Q Y, Kong H H, Jiang Y P, Gao Y W, Deng G H, Shi J Z, Tian G B, Liu L L, Liu J X, Guan Y T, Bu Z G, Chen H L. 2013. H5N1 hybrid viruses bearing 2009/H1N1 virus genes transmit in guinea pigs by respiratory droplet. *Science*, **340**, 1459–1463.

Zhu X Y, Yu W L, McBride R, Li Y, Chen L M, Donis R O, Tong S X, Paulson J C, Wilson I A. 2013. Hemagglutinin homologue from H17N10 bat influenza virus exhibits divergent receptor-binding and pH-dependent fusion activities. *Proceedings of the National Academy of Sciences of the United States of America*, **110**, 1458–1463.

Executive Editor-in-Chief CHEN Hua-lan
Managing editor ZHANG Juan